

RSC Advances



This is an *Accepted Manuscript*, which has been through the Royal Society of Chemistry peer review process and has been accepted for publication.

Accepted Manuscripts are published online shortly after acceptance, before technical editing, formatting and proof reading. Using this free service, authors can make their results available to the community, in citable form, before we publish the edited article. This *Accepted Manuscript* will be replaced by the edited, formatted and paginated article as soon as this is available.

You can find more information about *Accepted Manuscripts* in the [Information for Authors](#).

Please note that technical editing may introduce minor changes to the text and/or graphics, which may alter content. The journal's standard [Terms & Conditions](#) and the [Ethical guidelines](#) still apply. In no event shall the Royal Society of Chemistry be held responsible for any errors or omissions in this *Accepted Manuscript* or any consequences arising from the use of any information it contains.

Efficient mixed metal oxides routed synthesis of boron nitride nanotubes

Jeghan Shrine Maria Nithya^a and Arumugam Pandurangan^{a, b*}

^a Department of Chemistry, Anna University, Chennai–600025, Tamilnadu, India

^b Institute of Catalysis and Petroleum Technology, Anna University, Chennai–600025,
Tamilnadu, India

*Corresponding Author: E-mail ID: pandurangan_a@yahoo.com

Tel: +91–44–22358653; Fax: +91–44–2220060

Abstract

Boron nitride nanotubes (BNNTs) were successfully synthesized by a simple annealing process. Amorphous boron powder (B) was used as boron source to react with various metal oxide mixtures (V_2O_5/Fe_2O_3 and V_2O_5/Ni_2O_3). V_2O_5 act as an efficient promoter in the synthesis process due to its high oxidizing and reducing properties. The Fe_2O_3 and Ni_2O_3 perform the role of catalyst in combination with B/ V_2O_5 system in achieving high crystalline BNNTs at 1100°C. The morphology and crystalline nature of the BNNTs were characterised by transmission electron microscopy, X-ray diffraction and Raman spectroscopy. The observations revealed the hexagonal-BN (h-BN) phase of BNNTs with high crystalline tubular structure. This method proved to be simple and economical using B/ V_2O_5/Fe_2O_3 and B/ V_2O_5/Ni_2O_3 mixtures for the large scale production of BNNTs.

KEYWORDS: Nanotubes, Thermal annealing, boron nitride and Chemical Vapor deposition.

1. INTRODUCTION

One dimensional (1D) nanomaterials including nanotubes, nanowires, nanorods and nanobelts have drawn extensive attention in various areas such as electronic, electrical pharmaceutical, cosmetics and biomedical applications.¹⁻² Among various 1D nanostructures, the most exciting class of nanotubes are carbon nanotubes (CNTs) and boron nitride nanotubes (BNNTs). Owing to their structural similarities, BNNTs possesses several advantages over CNTs.³ BNNTs exhibit excellent mechanical, electrical and electronic properties, thermal stability, oxidation resistivity and wide band gap independent of geometrical parameter.⁴ The theoretical view of BNNTs were first proposed by Rubio et al in 1994 and in the sub-sequent year BNNTs production was achieved by Chopra et al.^{5, 6}

The most popular methods such as arc-discharge, laser ablation, ball milling, template assisted synthesis and plasma jet failed to synthesis BNNTs with high purity and high yield.⁷ Chemical vapor deposition (CVD) technique is considered to be a simple method for the production of BNNTs using various liquid precursors diborane (B_2H_6), borazine ($B_3N_3H_6$) and trimethyl borate ($C_3H_9BO_3$).⁸⁻¹¹ The drawback in this reaction process is the in-situ generation of liquid vapors. To date, the boron oxide chemical vapor deposition (BOCVD) method yields large quantity of BNNTs. This method mainly utilizes MgO as support (B/MgO, B/MgO / Fe_2O_3 and B/MgO/SnO) for the growth of BNNTs.¹² Pakdel et al (2012) reported the formation of well structured BNNTs by annealing B/FeO/MgO.¹³ Further, Ozmen et al (2013) explained the formation of BNNTs over amorphous B and Fe_2O_3 .¹⁴ Li et al (2011) have reported the synthesis of BNNTs over stainless steel substrate by annealing amorphous B and Fe_2O_3 .¹⁵

Apart from using metal oxide as supports, there are also reports for the production of BNNTs using self propagation high temperature synthesis (SHS) method,¹⁶ formation of

multi-walled and double walled BNNTs by the catalytic CVD (CCVD) aided with a floating nickel catalyst,¹⁷ A nano-template reaction, using single-wall carbon nanotubes (SWCNTs) as template and ammonia borane complexes (ABC) precursors was also reported by Nakanishi et al.¹⁸ Colemanite ($\text{Ca}_2\text{B}_6\text{O}_{11}\cdot 5\text{H}_2\text{O}$) mixed with ZnO, Al_2O_3 , Fe_3O_4 , and Fe_2O_3 also produced BNNTs.¹⁹ However, all these reported approaches have various disadvantages either with the selection of precursors with complex operational equipment setup and or growth temperature $> 1200^\circ\text{C}$. In the current scenario, the demand of BNNTs synthesis in large scale is considered a necessity for various commercial applications in catalysis, drug delivery, storage, nano encapsulation, transport of various molecules and medical diagnosis.²⁰⁻²²

In order to elucidate the above problems the present investigation focuses on BNNTs preparation relatively at lower temperature with simple process compared to existing approaches. In this context, thermal CVD method was selected for the production of high quantity of BNNTs by heating boron with metal oxides. Here we have investigated a pair of reaction mixtures B/ $\text{V}_2\text{O}_5/\text{Fe}_2\text{O}_3$ or B/ $\text{V}_2\text{O}_5/\text{Ni}_2\text{O}_3$ for the synthesis of BNNTs. V_2O_5 that can act as promoter, oxidizer and support is introduced in the reactions. The motivation for the selection of V_2O_5 lies behind the creative work of Goldberg et al.²³ Fe_2O_3 and Ni_2O_3 are selected as catalyst due to their high catalytic efficiency towards nanotube formation.²⁴ Metastable Ni_2O_3 was chosen because it can be easily reduced to NiO or Ni which leads to the formation of BNNTs at lower temperature.²⁵ Already our group were successful in the production of BNNTs using MoO_3 as an promoter using Fe_2O_3 and Ni_2O_3 as catalyst.²⁶

In the present investigation, V_2O_5 undergo reduction and also oxidize boron at low temperature. Simultaneously, boron reacts with $\text{Fe}_2\text{O}_3/\text{Ni}_2\text{O}_3$ and generates B_2O_2 vapors. The large amount of B_2O_2 vapors formed during this process reacts with NH_3 , forming BN. Fe/Ni

which attains liquid state, facilitates the formation of BNNTs. The color of the amorphous boron mixture ($B/V_2O_5/Fe_2O_3$ and $B/V_2O_5/Ni_2O_3$), changes from dark brown to white and this observation further confirms the formation of BNNTs. The effect of reaction temperature on the growth of BNNTs was studied and morphological changes, such as the tube structure and tube diameter were also investigated using TEM studies. The role of V_2O_5 in the synthetic process, were also explained in detail.

2. EXPERIMENTAL

2.1 Materials

Amorphous boron powder (Loba Chemie. Pvt. Ltd), Fe_2O_3 (Central Drug House), V_2O_5 and Ni_2O_3 (Sisco Research Laboratories Pvt. Ltd) were purchased and used as such. NH_3 and N_2 gases were used as the N source and carrier gas, respectively.

2.2 Synthesis of Boron Nitride Nanotubes

In this synthesis, a simple annealing process was adopted as reported by Tang et al.²⁷ The reactions were performed in a horizontal tubular furnace, consisting of an alumina tube. The reactant mixtures, $B/V_2O_5/Fe_2O_3$ or $B/V_2O_5/Ni_2O_3$ were mixed adequately with the weight ratio 2:1:1 and loaded in an alumina boat. The boat was placed at the center of the tubular furnace. The ends of the alumina tube were closed with steel lids, carrying a gas inlet and outlet. Initially, the furnace was programmed with a ramp rate of $5^\circ C/min$ and heated to $900^\circ C$ in N_2 gas flow (50 sccm) to eliminate the residual air. Then the temperature was raised to $1000-1200^\circ C$ and maintained for 1 h in NH_3 atmosphere (50 sccm). After the completion of the reaction time, the furnace was slowly cooled to room temperature under N_2 atmosphere. The as-synthesized samples were weighed and purified by stirring with 2M HCl solution for 6 h at room temperature. The product was further treated with 1M HNO_3 for 24 h

at 50°C, to remove all the metal particles and amorphous boron powder. Finally, it was filtered, washed with distilled water and dried at 100°C.²⁸

2.3 Characterization methods

Crystalline structure of the samples were investigated by X-ray diffraction (XRD) analysis using a Cu K α ($\lambda=1.54$ Å) radiation source at room temperature operated with 40 kV, 230 mA, at a scan rate of 0.02° (2 θ) per sec from 10 to 80° (2 θ). The Fourier transform–infrared (FT–IR) spectroscopy analyses were recorded on a Perkin Elmer spectrophotometer. The morphological changes of the samples were studied by scanning electron microscopy (SEM, JEOL–840) and their elemental compositions were identified with energy dispersive spectroscopy (EDS). Nanostructures were viewed by transmission electron microscopy (TEM, JEOL–2100) instrument operated at 200 kV. In the analysis, the samples were ultrasonically dispersed in acetone and dropped onto a carbon–coated copper grid. Raman spectroscopy analysis was plotted on WITec alpha 300R with the 532 nm laser line from Nd: YAG source. X-ray photoelectron spectroscopy (XPS) analysis was performed using Omicron Nanotechnology GMBH spectrometer employing monochromatic AlK α (1486.6eV) X-ray source. According to the binding energy of carbon (C-C) at 284.6 eV, all the XPS profile are corrected.

3. RESULTS AND DISCUSSION

3.1 Structural and Morphological Studies on BNNTs

3.1.1 X-ray Diffraction Analysis

The crystalline natures of BNNTs were examined by XRD analysis. Fig.1 (a-c) represents the XRD patterns pretending to purified BNNTs obtained during the reaction using B/V₂O₅/Fe₂O₃ and NH₃ at various temperatures 1000, 1100 and 1200°C. The as-synthesised

product obtained at 1100°C in Fig.1 (Inset pattern) clearly shows the mixture of phases, such as hexagonal BN (h-BN), VO₂, VO and Fe. The peaks related to VO₂ is inferred from XRD pattern around 2θ of 31.5°, 33.3°, 35.5° and 65.06° (JCPDS no: 82-1074). The peaks at 2θ of 37.7° and 44.67° confirms VO phase (JCPDS no: 77-2173). The formation of VO₂ and VO is due to the reduction of V₂O₅. During annealing process, the reduction of Fe₂O₃ to Fe occurred completely. The presence of Fe is observed around 2θ of 43.6° and 63.7° (JCPDS no: 89-4186). The peaks at 2θ of 26.67°, 41.85°, 53.59° and 76.38° corresponds to h-BN phase. The formation of h-BN is due to the oxidation of B and the reduction process of V₂O₅/Fe₂O₃.

The XRD patterns in Fig. 1(a–c) show the reflections of h-BN phase at (002), (100), (101), (102), (004), (104) and (110). It is also observed, the crystallinity of h-BN phase is increased with increase in temperature. In Fig.1b, the diffraction of h-BN at 2θ of 26.5°, 41.7°, 43.5°, 50.6°, 54.6°, 72.5° and 75.6° corresponds to inter-planar spacing of 3.36, 2.16, 2.07, 1.80, 1.67, 1.30 and 1.25 Å respectively. The calculated lattice constant values, a = 2.49 and c = 6.72 Å are consistent with JCPDS file no: 85–1068.

Fig. 2 shows the XRD pattern of the BNNTs, formed over B/V₂O₅/Ni₂O₃ at 1000, 1100 and 1200°C. The inset XRD pattern represents the as-synthesized product obtained at 1100 °C. This XRD pattern evidenced the peaks related to h-BN, NiO, Ni, VO₂ and VO. The formation of NiO and Ni phase is due to the reduction of Ni₂O₃. The characteristic peak at 2θ of 37.3° and 43.2° corresponds to NiO phase (JCPDS file no: 89-3080). Similarly, the peak at 2θ of 44.4° relates to Ni (JCPDS file no: 88-2326). The presence of other two phases, VO₂ and VO is due to the reduction of V₂O₅ which was observed same as in the case of B/V₂O₅/Fe₂O₃. The diffraction peaks at 2θ of 26.29°, 42.4° and 76.38° shows the finger print of h-BN phase.

Fig.2 (a-c) represents the XRD pattern of purified BNNT formed over B/V₂O₅/Ni₂O₃. The entire diffraction pattern depicts the formation of (002), (100), (004), (104) and (110) planes related to h-BN. It is observed that the peaks related to metal oxide was totally absent. Noteworthy, the intensity of h-BN phase increases with increase in temperature. In Fig.2b the calculated d-spacing value 3.39, 2.17, 1.68, 1.30 and 1.25 Å refers to (002), (100), (004), (104) and (110) planes respectively. The lattice constants, a=2.50 and c=6.77Å, were found to be matched with JCPDS file no: 34-0421.

The presence of Fe₂O₃ and Ni₂O₃ in the reactant mixture plays a vital role in the formation of BNNTs. In general, Fe and Ni catalyze the reaction and influence the formation of BNNT. In this study, Fe₂O₃ and Ni₂O₃ completely reduce to Fe and Ni respectively. Although NiO is more stable than Ni₂O₃, the formation of Ni by reduction is more possible at lower temperature while using Ni₂O₃.²⁵

3.1.2 Scanning Electron Microscopy Analysis

The effect of various reaction temperatures at 1000, 1100 and 1200°C on the growth of BNNTs over B/V₂O₅/Fe₂O₃ and B/V₂O₅/Ni₂O₃ was studied. Fig. 3(a-c) illustrates the SEM images of as-synthesised BNNTs obtained at various temperatures using B/V₂O₅/Fe₂O₃. At 1000°C, the formation of bulk BN dominates the BNNTs formation. According to the thermodynamic study, VO₂ were found to be in liquid state above 953°C.²⁹ At this state liquid VO₂/B/Fe₂O₃ (solid) would mix with each other; this initiates the reduction of Fe₂O₃ to Fe and also oxidizes B to B₂O₂ at earlier stage. The reaction between B₂O₂ and NH₃ initially creates B/N species and the development in the growth phase resulted in the formation of coiled like structure was shown in Fig. 3a. when the temperature was raised to 1100°C, the nucleation of BN occurs on the surface of finely dispersed Fe particles and upon supersaturation, BN shells gets precipitated layer by layer.¹³ At this stage, morphology of

BNNTs were observed to be straight than as coiled structures, as shown in Fig. 3b. Similar characteristics of the BNNTs were also reflected at 1200°C (Fig. 3c). So, based on these results, it is well understood that 1100°C yield high quality BNNTs than 1000°C. The EDS spectrum shown in Fig. 3d represents the elemental composition of BNNT obtained at 1100°C. The peak confirmed the existence of B and N in the sample.

Similarly, the SEM images of as-synthesised products obtained using B/V₂O₅/Ni₂O₃ where studied at various temperatures 1000, 1100 and 1200°C is shown in Fig 4. It was observed that the BNNTs were grown at 1000°C. The theoretical background in this reaction process states that the metastable Ni₂O₃ started to decompose at 600°C and attained liquid to solid state (NiO) at earlier stage. As stated earlier, V₂O₅ decomposed to VO₂ and VO and attained liquid state above 953°C. Both these reduction reactions in turn oxidize boron and generate enormous amount of B₂O₂ vapors. When the temperature reaches 1000°C, these B₂O₂ vapors reacts with NH₃ gas and promote the precipitation of BN over the Ni catalyst. The nucleation process initiates the growth of nanotubes by layer deposition on the surface of catalyst which tends to form BNNTs as shown in Fig. 4a. Maximum yield of BNNTs were obtained at 1100°C compared to other temperature. Fig. 4d represent the EDS spectrum of BNNT obtained depicts the presence of B and N. The additional peaks in Fig.4d have their origin from unreacted species.

3.1.3 Transmission Electron Microscopy Analysis

The morphologies of the BNNTs synthesised from the B/V₂O₅/Fe₂O₃ at 1100°C were analyzed by TEM as shown in Fig. 5. The morphologies of the tubes were observed to be multiwalled. Fig. 5a represents the TEM image of as-synthesised BNNTs. It is clearly evidenced that the tubes were grown from the solid support. The morphologies of the purified BNNTs were displayed in the Fig. 5(b-e). The selected area electron diffraction (SAED)

pattern in Fig. 5d (insert image), taken from the central part of the nanotubes, corresponds to (002), (100), (101), (104) and (110) of hexagonal BN. The crystalline nature of BNNTs formed at 1100°C confirmed by the SAED pattern is consistent with XRD pattern. It was observed from Fig. 5e; the BNNTs possess inner and outer diameters of 7.67 and 17.2 nm, respectively.

The morphology of BNNTs synthesised from B/V₂O₅/Ni₂O₃ at 1100°C were studied by TEM analysis as shown in Fig. 6. The TEM images of the as-synthesised BNNTs are shown in Fig. 6a. We can notice from the Fig.6a, that the tubes are straight in shape and had originated from the support. These tubes were comparatively longer with a smaller diameter, than the tubes formed over B/V₂O₅/Fe₂O₃. Fig. 6 (b-e) denotes the TEM images of purified BNNTs taken at various magnifications. The length of the tubes was found to be >1 μm. The bunch of BNNTs and multi-walled layers can be clearly identified from the TEM images. The tubes had both opened and closed ends. The inset SAED pattern shown in Fig. 6c corresponds to crystalline planes of the h-BN structure (002), (100), (004), (104) and (110) which coincide with the XRD analysis. These results confirm the formation of high crystalline BNNTs. The BNNTs obtained in our case were similar in morphology as reported by Zhi et al.³⁰ The inner and outer diameters of the tubes were found to be 5.16 and 10.96 nm, respectively.

3.1.4 Fourier Transform–Infrared Spectroscopy Analysis

The FT-IR spectra of the purified BNNTs formed over B/V₂O₅/Fe₂O₃ and B/V₂O₅/Ni₂O₃ at 1100°C are shown in Fig. 7. The spectra indicate the formation of h-BN. The two broad peaks at 1384 and 1382 cm⁻¹ correspond to the B–N stretching vibrations, and the sharp peaks centered at 788 and 786 cm⁻¹ were due to the B–N–B bending vibrations.^{31, 32} The peak at 2300 cm⁻¹ was assigned to boron and at 2518 cm⁻¹ was due to CO₂ adsorption from the

surface atmosphere. The weak bands at 3412 and 3413 cm^{-1} was due to the O-H stretching vibrations of water.^{14, 33}

3.1.5 Raman Spectroscopy Studies

The crystalline natures of BNNTs were further analyzed by the Raman spectra. Fig. 8a and b correspond to the Raman spectra of purified BNNTs formed over B/V₂O₅/Fe₂O₃ and B/V₂O₅/Ni₂O₃ at 1100°C. Both the spectra exhibit only one sharp peak at 1367 cm^{-1} . The peak corresponds to the in-plane vibrational Raman active E_{2g} mode of h-BN. In this mode, the B and N atoms were moving against each other within a plane. Lee et al, have also reported the similar observation for the BNNTs synthesized from B, MgO and FeO mixtures.³⁴ This result confirms that purified BNNTs were crystalline and free from impurities.

3.1.6 X-Ray Photoelectron Spectroscopy Analysis

The binding natures of h-BN in BNNTs were investigated using XPS spectroscopy. Fig.9 represents XPS spectrum of the purified BNNTs obtained using B/V₂O₅/Fe₂O₃ at 1100°C. The XPS spectra corresponding to purified BNNTs obtained from B/V₂O₅/Ni₂O₃ were shown in Fig. 10. The presences of carbon and oxygen spectrum in both the cases are due to the surface contamination during the exposure of the sample in the air before analysis.³⁵ The survey spectrum in the Fig. 9a shows the presence of boron and nitrogen in BNNTs. Fig. 9b shows the XPS profile related to B 1s at 190.7 and 188.2 eV. These peaks were ascribed to B-N bonding. The XPS spectra responsible for N 1s peak is shown in Fig. 9c. The origin of the peaks at 398.4 eV and 396.7 eV can be associated with the N atoms in N-B bond of typical h-BN species, as reported in the literature.^{36, 37}

Fig. 10a shows the survey spectrum of BNNTs formed over B/V₂O₅/Ni₂O₃. This indicates the presence of boron and nitrogen in the BNNT. The individual spectra of boron and nitrogen are shown in Fig. 10b and c, respectively. The peak at 190.1 and 188.9 eV corresponds to B 1s band attributed to B-N bonding. The N 1s peak at 397.9 and 396.5 eV assigned to N-B bonding of h-BN.³⁸

3.1.7 Yield and Purity of the Synthesized BNNTs

The yield and purity of the BNNTs grown from of B/V₂O₅/Fe₂O₃ and B/V₂O₅/Ni₂O₃ at 1100°C were summarized in Table 1. About 0.805 g of the reactant mixture (B/V₂O₅/Fe₂O₃) yielded 0.836 g of product after reaction. Consequently, after acid purification 0.818 g of BNNTs was obtained. Similarly, 0.802 g fine mixtures of B/V₂O₅/Ni₂O₃ produced 0.846 g of product followed by 0.834 g after acid purification. The percentage of yield after purification was found to be 97.8 and 98.5 % in case of B/V₂O₅/Fe₂O₃ and B/V₂O₅/Ni₂O₃, respectively. The results obtained from XRD, TEM, Raman and XPS analysis accounts for the purity of the formed nanotubes. The XRD patterns of purified BNNTs in the Figs. 1 and 2 clearly shows the hexagonal BN phase of the nanotubes formed, and this was further confirmed by the Raman spectra with the E_{2g} vibrational mode of h-BN. The TEM images of BNNTs evidenced that BNNTs were free from impurities. Consequently this also confirms the formation of pure BNNTs.

3.1.8 Catalytic activity and its influence on the growth of BNNTs

The catalytic activity of Fe₂O₃ and Ni₂O₃ on the growth of BNNTs was investigated by the addition of V₂O₅. When the reaction mixtures composed of B/V₂O₅/Fe₂O₃ were subjected to heating, V₂O₅ first started to melt at 690°C.³⁹ The thermodynamic study of VO₂-V₂O₅ suggest V₂O₅ is reduced to VO₂ at higher temperature. It was reported that at 953–1081°C,

liquid and solid curves of VO₂ exists.²⁹ Due to the low decomposition temperature the reduction of V₂O₅ was achieved by a combination of diffusion, coalescence and stabilization process⁴⁰. In this study, at 900°C, NH₃ gas was passed to reduce V₂O₅ to VO₂ and VO. Similarly, Fe₂O₃ was also reduced to Fe as shown in equation A1. The presence of Fe, VO₂ and VO were confirmed by XRD analysis. Both of these reduction processes enhances the oxidation of boron to form B₂O₂ vapors. Based on vapor-liquid-solid (V-L-S) mechanism, it was suggested that B/N nucleation process occurred when B₂O₂ vapors started to react with NH₃ and leads to the formation of the BN at initial stage.⁴¹ When the temperature was raised from 1000-1200°C, B₂O₂ vapors generated get reacted with NH₃ to form BNNTs as predicted by previous reports. Such processes facilitated the formation of BNNTs.⁴² Here, we suggest that the B₂O₂ vapors might have reacted with NH₃ to form intermediate HO-B=N-H vapors, as shown in equation A2. These vapors might be adsorbed and activated by the Fe/Ni clusters in the molten liquid to form BNNTs. The clusters decomposed HO-B=N-H to form BN, which might subsequently react on the catalyst surface to form BNNTs.



Also the mechanism for the formation of BNNTs from B/V₂O₅/Ni₂O₃ was similar to above process, except the formation of NiO and Ni. The formation of NiO and Ni was confirmed by XRD. Hence, this study establishes that V₂O₅ is an efficient oxidizing agent.

4. Conclusion

A simple annealing approach was developed to synthesize BNNTs by CVD. These BNNTs have distinct characteristics with controlled diameter and longer in length. The formed BNNTs were found to be h-BN with high crystallinity. This method can be extended to synthesize various BN based nanostructures. The synthesized BNNTs can be used as a nanovector in future due to its non-toxic nature.

Acknowledgements

One of the authors, Jeghan Shrine Maria Nithya is thankful to the AICTE for the award of the NDF (National Doctorial Fellowship) and also to the Department of Chemistry, for providing the facilities sponsored by the DST (FIST).

References

- [1] Y. Chen, C. P. Li, H. Chen and Y. Chen, *Sci Technol Adv Mat*, 2006, **7**, 839-846.
- [2] Z-G. Chen, J. Zou, G. Liu, F. Li, Y. Wang, L. Wang, X-L. Yuan, T. Sekiguchi, H-M. Cheng, and G.Q. Lu, *ACS Nano*, 2008, **2**, 2183–2191.
- [3] I. Capek, *Adv Colloid Interface Sci*, 2009, 63-89.
- [4] C. Zhi, Y. Bando, C.C. Tang, S. Honda, K. Sato, H. Kuwahara and D. Golberg, *Angew Chem Int Ed*, 2005, **150**, 7932 -7935.
- [5] A. Rubio, J. L. Corkill and M. L. Cohen, *Phys Rev B*, 1994, 5081.
- [6] N. G. Chopra, R. J. Luyken, K. Cherrey, V. H. Crespi, M. L. Cohen, S. G. Louie and A. Zettl, *Science*, 1995, **49**, 966–967.
- [7] C. Zhi, Y. Bando, C.C Tang and D. Golberg , *Mat Sci Eng R*, 2010, **70**, 92–111.
- [8] L. Guo, R.N. Singh, *Physica E*, 2009, **41**, 448–453.
- [9] C.Y. Su, Z.Y. Juang, K.F. Chen, B.M. Cheng, F.R. Chen, K.C. Leou, C.H. Tsai, J. *Phys Chem C*, 2009, **113**, 14681–14688.
- [10] O.R. Lourie, C.R. Jones, B.M. Bartlett, P.C. Gibbons, R.S. Ruoff, W.E. Buhro, *Chem Mater*, 2000, **12**, 1808–1810.
- [11] M.J. Kim, S. Chatterjee, S.M. Kim, E.A. Stach, M.G. Bradley, M.J. Pender, L.G. Sneddon, B. Maruyama, *Nano Lett*, 2008, **8**, 3298–3302.
- [12] J. Wang, C.H. Lee and Y.K. Yap, *Nanoscale*, 2010, **2**, 2028-2034.
- [13] A. Pakdel, C. Zhi, Y. Bando, T. Nakayama and D. Golberg, *Nanotechnology*, 2012, **23**, 215601.
- [14] D. Ozmen, N. A. Sezgi and S. Balci, *Chem. Eng. J*, 2013, **219**, 28–36.
- [15] J. Li , H. Lin, Y. Chen, Q. Su and Q. Huang, *Chem. Eng. J*, 2011, **174**, 687– 692.

- [16] J. Wang, L. Zhang, Y. Gu, X. Pan, G. Zhao, and Z. Zhang, *Mater Res Bull*, 2013, **48**, 943–947.
- [17] S. Chatterjee, M. J. Kim, D. N. Zakharov, S. M. Kim, E. A. Stach, B. Maruyama, and L. G. Sneddon, *Chem. Mater*, 2012, **24**, 2872–2879
- [18] R. Nakanishi, R. Kitaura, J. H. Warner, Y. Yamamoto, S. Arai, Y. Miyata and H. Shinohara, *Sci. Rep*, 2013, **3**, 1385.
- [19] S. Kalay, Z. Yilmaz and M. Culha, *Beilstein J. Nanotechnol*, 2013, **4**, 843-851.
- [20] M. Corrias, B. Caussat, A. Ayrat, J. Durand, Y. Kihn, Ph. Kalck and Ph. Serp, *Chem Eng Sci*, 2003, **58**, 4475-4482.
- [21] Z-G, Chen, J. Zou, Q. Liu, C. Sun, G. Liu, X. Yao, F. Li, B. Wu, X-L. Yuan, T. Sekiguchi, H-M. Cheng and G.Q. Lu, *ACS Nano*, 2008, **8**, 1523-1532.
- [22] R. H. Baughman, A. A. Zakhidov and W. A. D. Heer, *Science*, 2002, **297**, 787-792D.
- [23] Golberg, Y. Bando and K. Kurashima, *Solid State Commun*, 2000, **116**, 1-6.
- [24] C-Y. Su, W-Y. Chu, Z-Y. Juang, K-F. Chen, B-M. Cheng, F-R. Chen, K-C. Leou and C-H. Tsai, *J. Phys. Chem. C*, 2009, **113**, 14732–14738.
- [25] S. Yang and J.-S. Kim, *J. Korean Phys. Soc*, 2010, **56**, 659-665
- [26] J.S.M. Nithya and A. Pandurangan, *J Nanosci Nanotechnol*, 2012, **12**, 1-7.
- [27] C.C. Tang, M.L. de la chapelle, P. Li, Y.M. Liu, H.Y. Dang and S.S. Fan, *Chem Phys Let*, 2001, **342**, 492-496.
- [28] T. Oku, N. Koi, K. Suganuma, R.V. Belosludov and Y. Kawazoe, *Solid State Commun*, 2007,**143**, 331-336.
- [29] H. Suito and D. R. Gaskell, *Metall Trans B*, 1971, **2**, 3299.
- [30] C. Zhi, Y. Bando, C.C. Tan and D. Golberg, *Solid State Commun*, 2005,**135**, 67-70.
- [31] X. Chen, X. Wang, J. Liu, Z. Wang and Y. Qian, *Appl Phys*, 2005, **81**, 1035-1037.

- [32] C. Peijun, C. Luyang, S. Liang, Y. Zeheng, Z. Aiwu, G. Yunle, H. Tao and Q. Yitai, *Solid State Commun*, 2005, **133**, 621.
- [33] H. Yu, X. Huang, G. Wen, T. Zhang, B. Zhong and H. Bai , *Mater Chem Phys*, 2011, **129**, 30-34.
- [34] C.H. Lee, J. Wang, V.K. Kayatsha, J.Y. Huang and Y.K. Yap, *Nanotechnology*, 2008, **19**, 455605.
- [35] B. Zhong , L. Song , X.X. Huang , G.W. Wen and L. Xia, *Mater Res Bull*, 2011, **46**, 1521–1523.
- [36] C.D. Wagner: Handbook of X-ray Photoelectron Spectroscopy, Perkin–Elmer Corporation, Minnesota, 1979.
- [37] J. Li, J. Li, Y. Yin, Y. Chen and X. Bi, *Nanotechnology*, 2013, **24**, 365605.
- [38] A. Gomathi and C.N.R. Rao, *Mater Res Bull*, 2006, **41**, 941.
- [39] V.G. Samsonov, *The Oxide Handbook*, Plenum Press, NewYork, 1973.
- [40] D.S. Su and R. Schlögl, *Catal Lett*, 2002, **83**, 115-119.
- [41] R. S. Wagner and W. C. Ellis, *Appl Phys Lett*, 1964, **4**, 89-90.
- [42] C.C. Tang, S.S. Fan, P. Li, Y.M. Liu and H.Y. Dang, *Mater Lett*, 2001, **51**, 315-319.

Table caption

Table. 1. Summary of Characterization techniques: indicating yield and the purity of BNNTs.

Figure captions

Fig.1. XRD patterns of BNNTs formed over B/V₂O₅/Fe₂O₃ at (a) 1000°C, (b) 1100°C, (c) 1200°C and insert XRD pattern of as-synthesized sample obtained at 1100°C.

Fig.2. XRD patterns of BNNTs formed over B/V₂O₅/Ni₂O₃ at (a) 1000°C, (b) 1100°C, (c) 1200°C and insert XRD pattern of as-synthesized sample obtained at 1100°C.

Fig.3. SEM images of BNNTs formed over B/V₂O₅/Fe₂O₃ at (a) 1000°C, (b) 1100°C and (c) 1200°C and (d) EDAX spectrum taken for BNNTs at 1100°C shown in image (b) .

Fig.4. SEM images of BNNTs formed over B/V₂O₅/Ni₂O₃ at (a) 1000°C, (b) 1100°C and (c) 1200°C and (d) EDAX spectrum taken for BNNTs at 1100°C shown in image (b).

Fig.5. TEM images of BNNTs formed over B/V₂O₅/Fe₂O₃ at 1100°C, low magnification image indicating as-synthesised BNNTs grows from solid precursors (a), high Resolution TEM images of purified BNNTs (b–e), selected area electron diffraction pattern taken from the tube surface inset in image (d).

Fig.6. TEM images of BNNTs formed over B/V₂O₅/Ni₂O₃ at 1100°C, low magnification image indicating as-synthesised BNNTs grown from solid precursors (a), high resolution TEM images of purified BNNTs (b–d) and corresponding selected area electron diffraction pattern taken from the tube surface, inset in image (d)

Fig.7. FT–IR spectra of purified BNNTs formed over B/V₂O₅/Fe₂O₃ (a) and B/V₂O₅/Ni₂O₃ at 1100°C (b).

Fig.8. Raman spectra of purified BNNTs formed over B/V₂O₅/Fe₂O₃ (a) and B/V₂O₅/Ni₂O₃ at 1100°C (b).

Fig.9. XPS spectrum of purified BNNTs formed over B/V₂O₅/Fe₂O₃ at 1100°C (a) the survey spectrum, (b) B1s and (c) N1s.

Fig.10. XPS spectrum of purified BNNTs formed over B/V₂O₅/Ni₂O₃ at 1100°C (a) The survey spectrum, (b) B1s and (c) N1s

Table 1

Samples	%. yield	XRD	TEM	Raman	XPS
B/V₂O₅/Fe₂O₃	97.8	h-BN phase	Inner dia- 7.67 nm Outer dia- 17.2 nm	h-BN	h-BN
B/V₂O₅/Ni₂O₃	98.5	h-BN phase	Inner dia- 5.17 nm Outer dia- 10.9 nm	h-BN	h-BN

Fig. 1

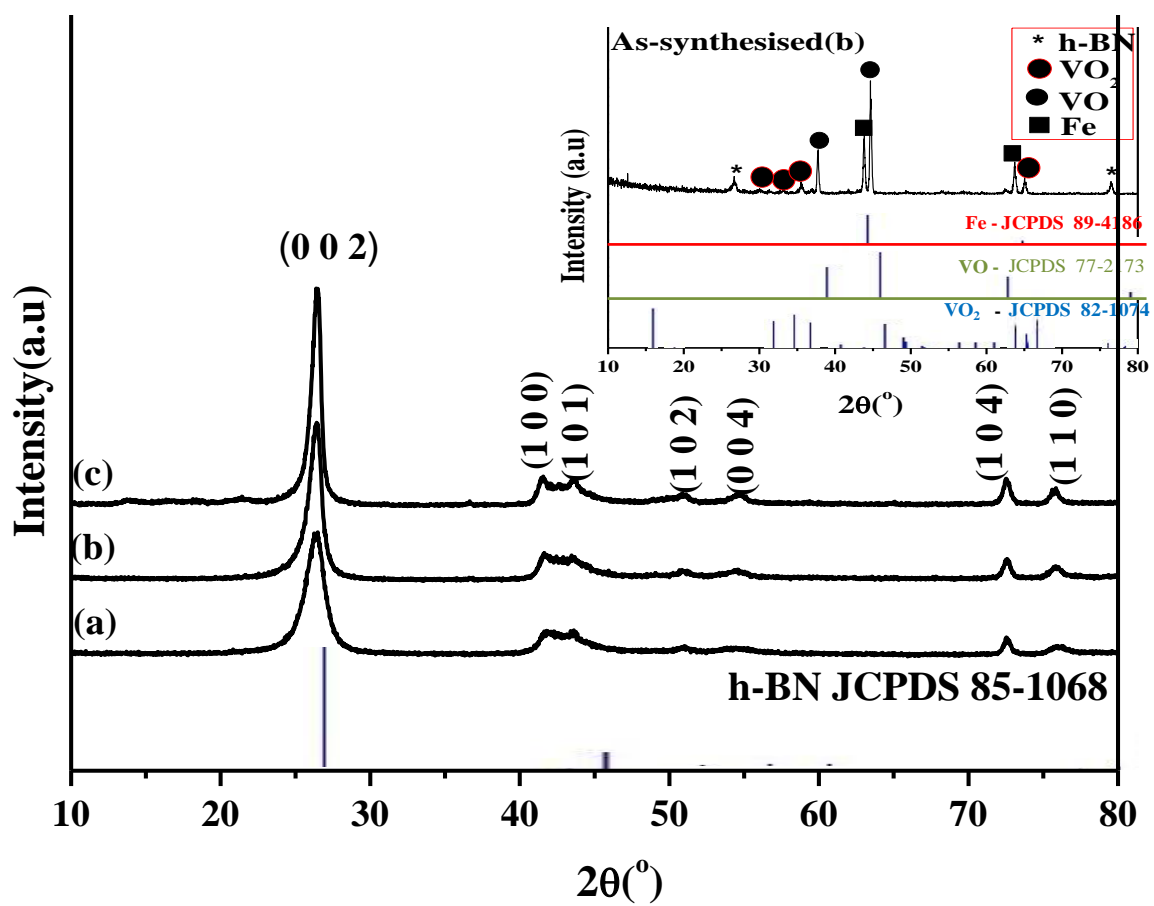


Fig. 2

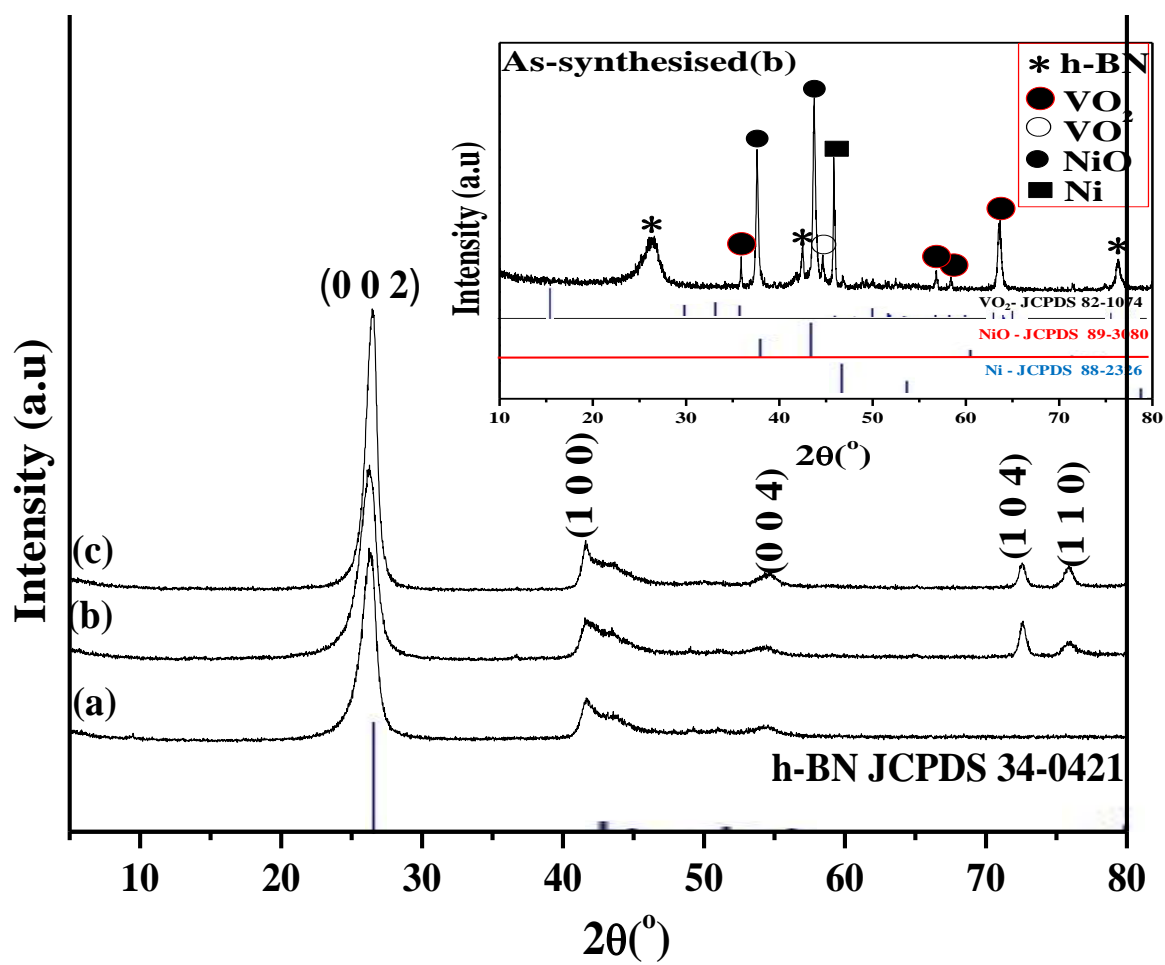


Fig. 3

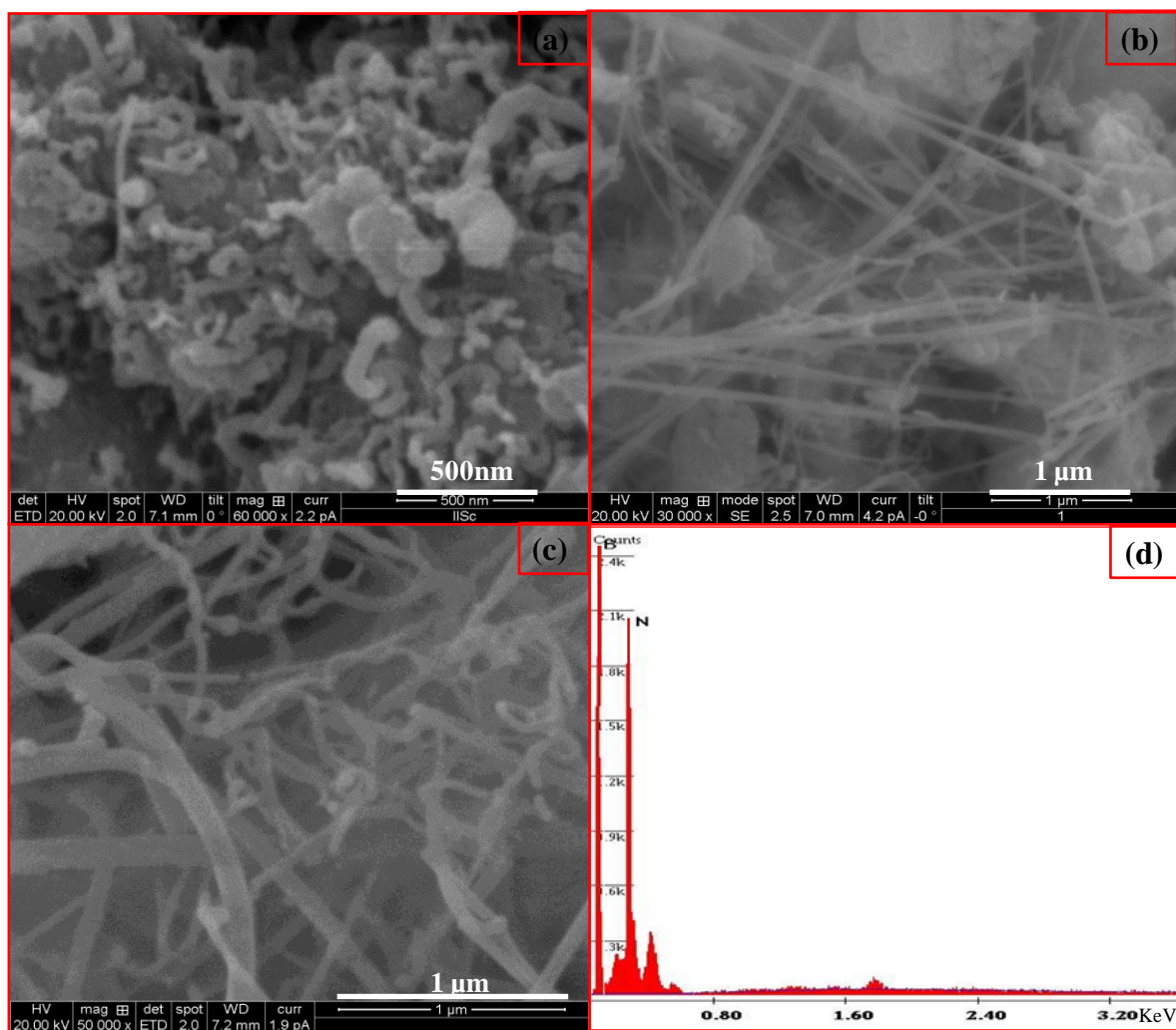


Fig. 4

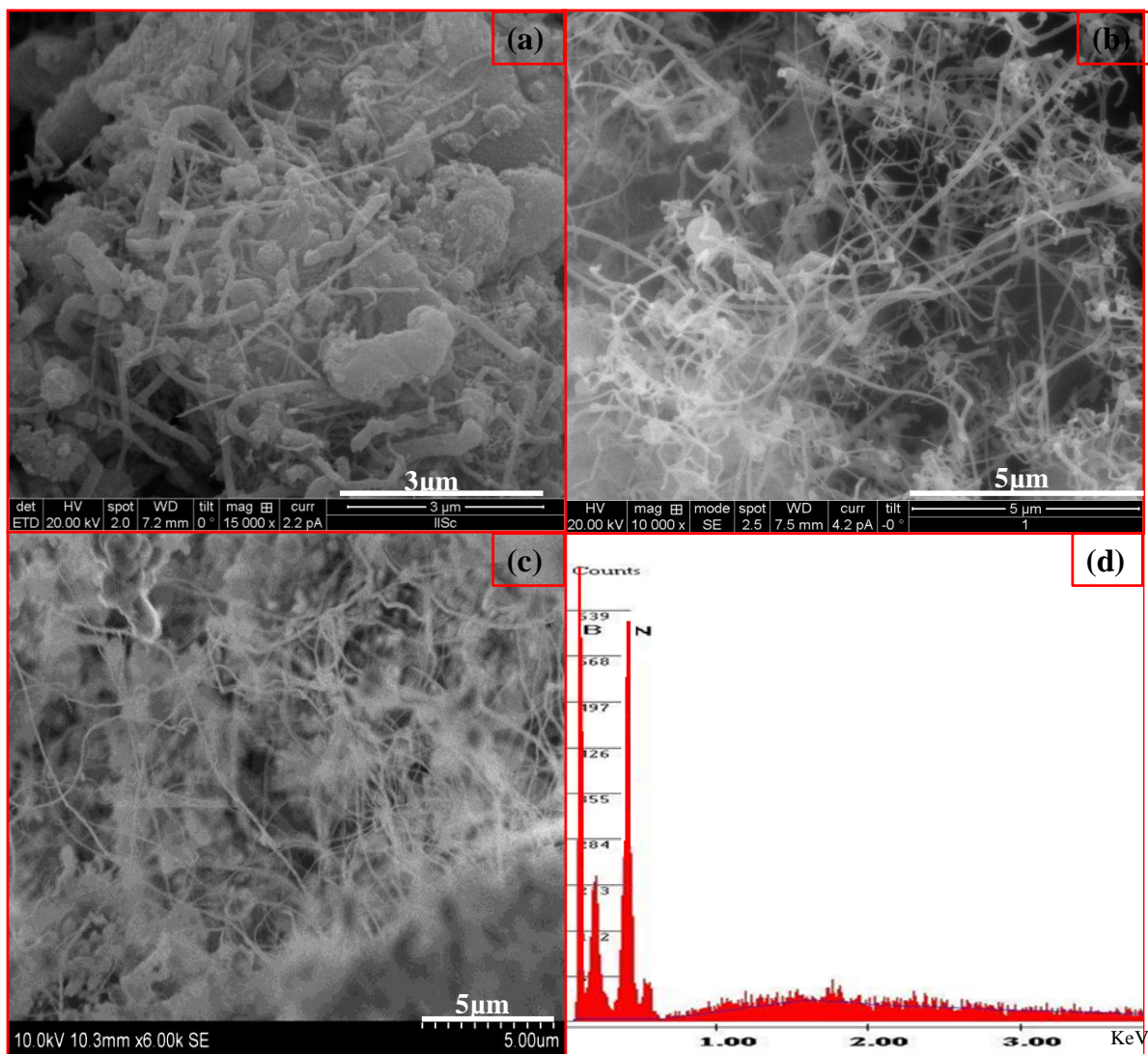


Fig. 5

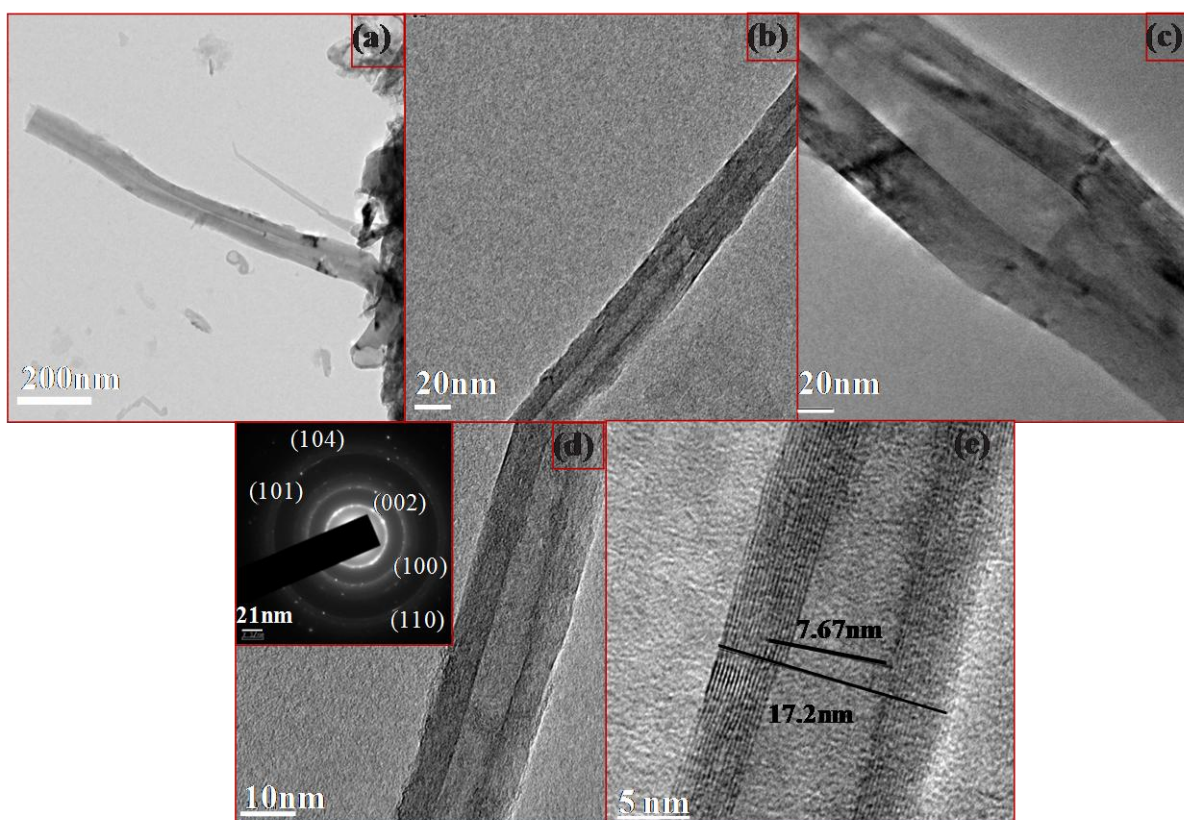


Fig. 6

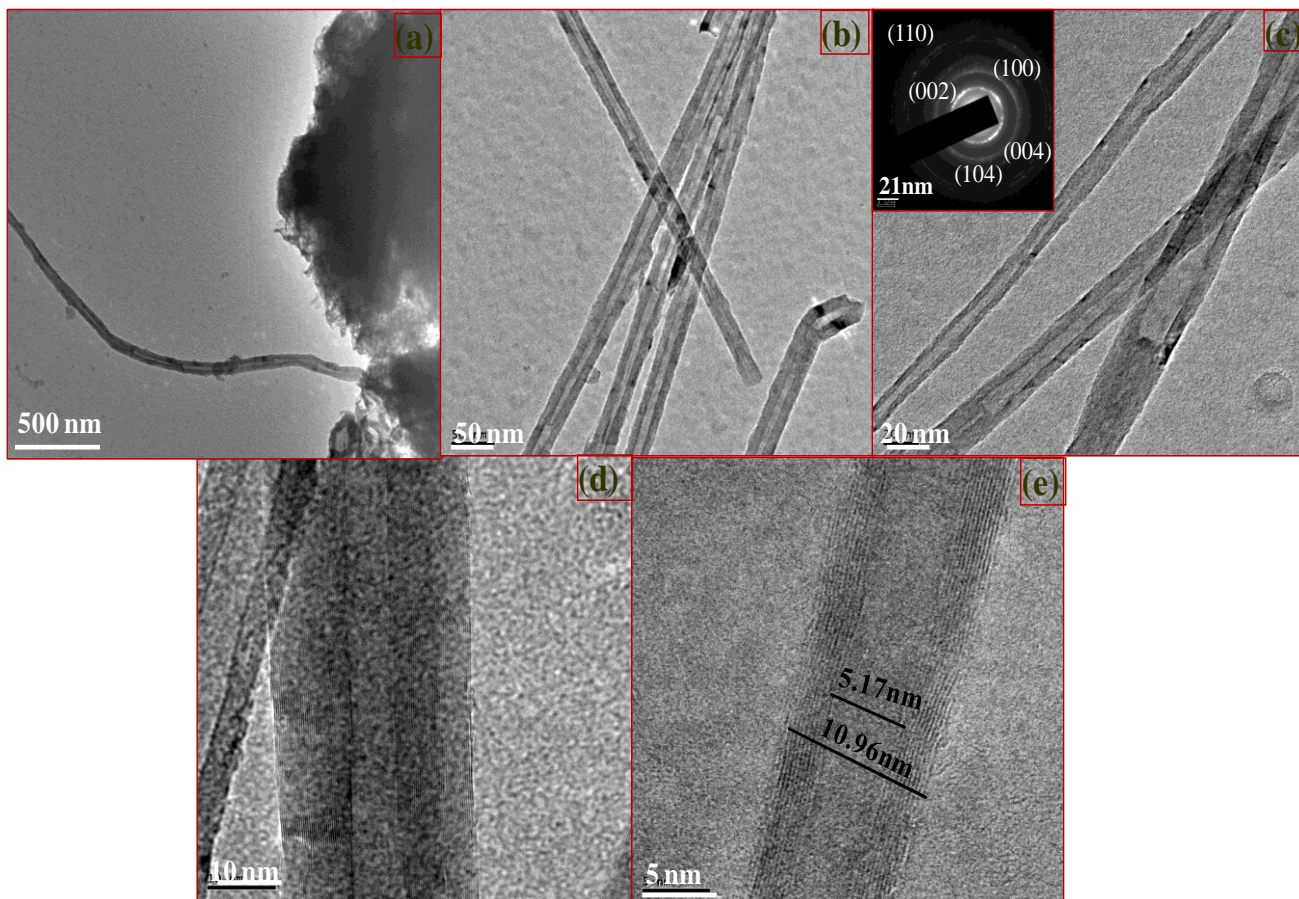


Fig. 7

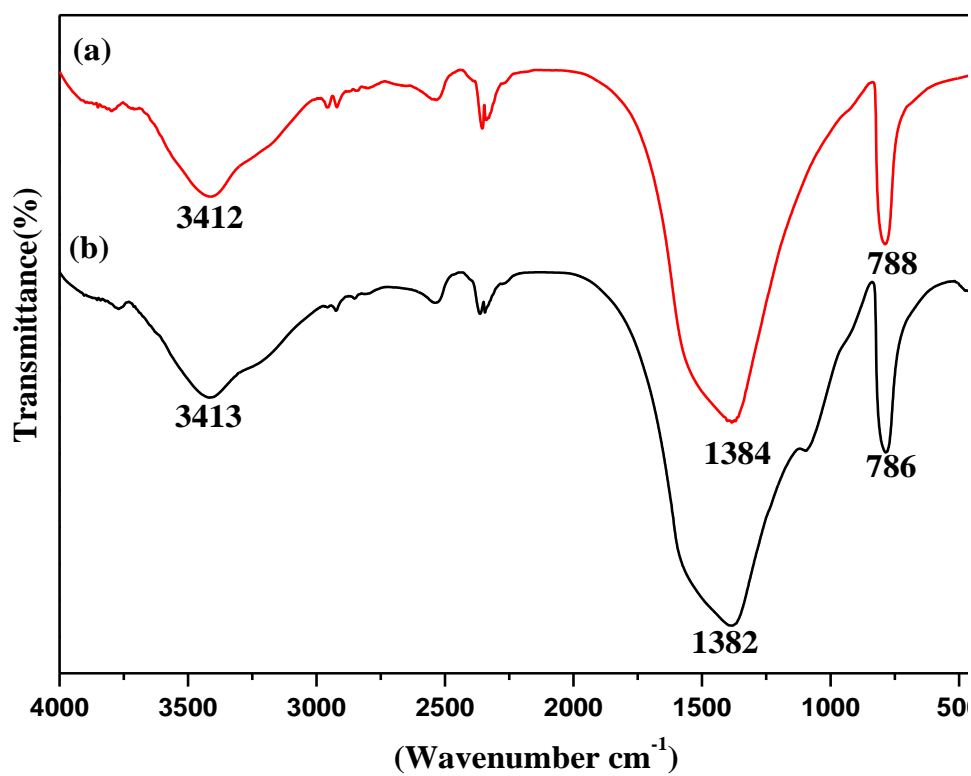


Fig. 8

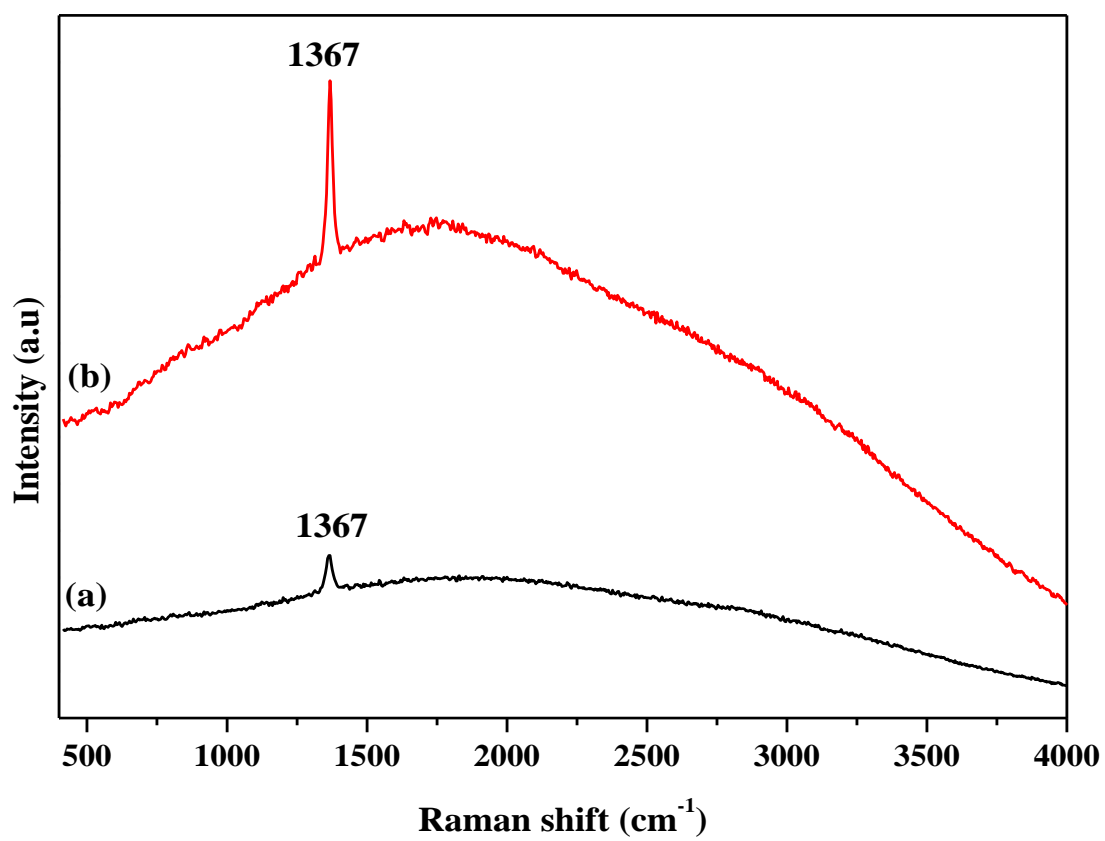


Fig. 9

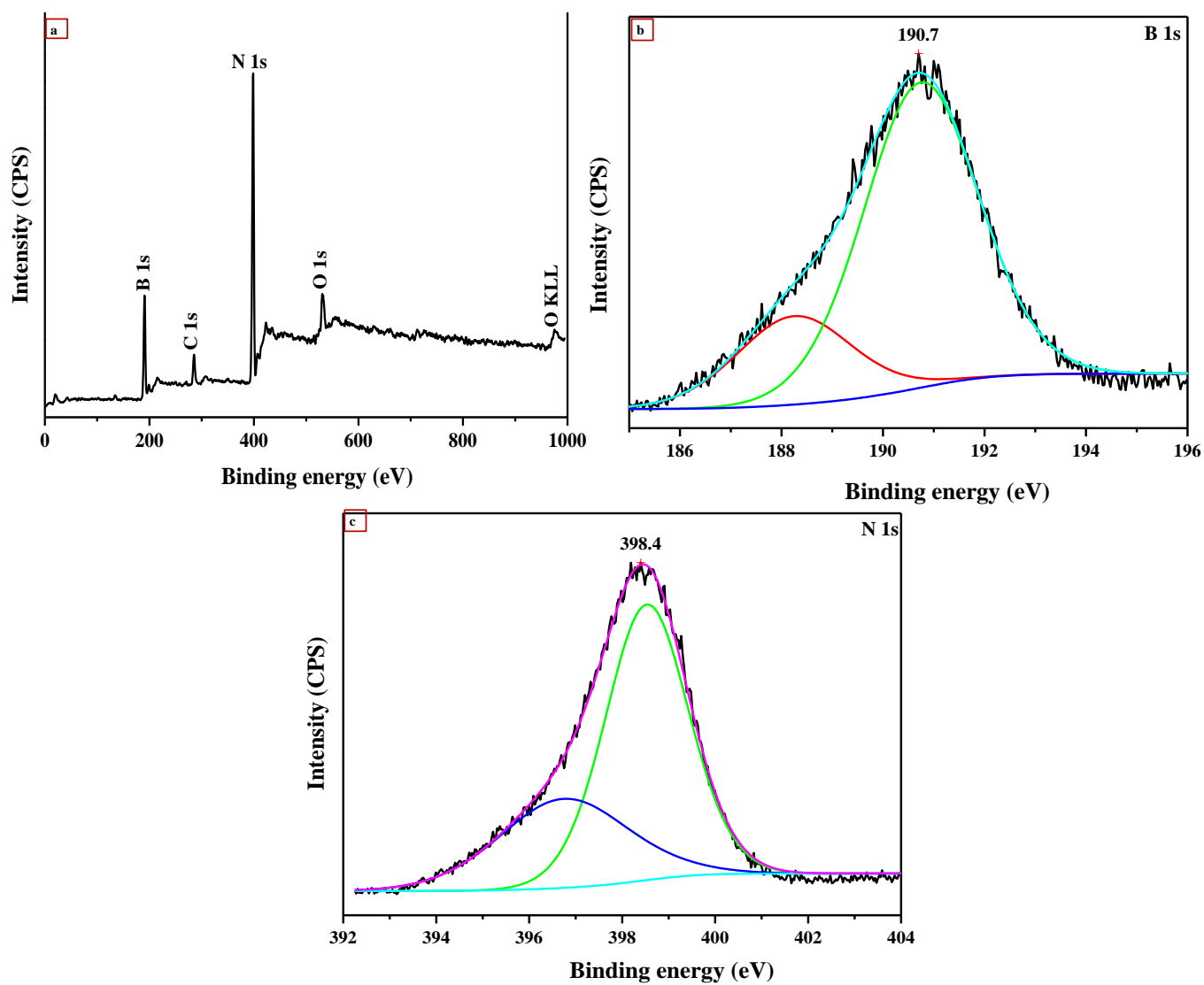
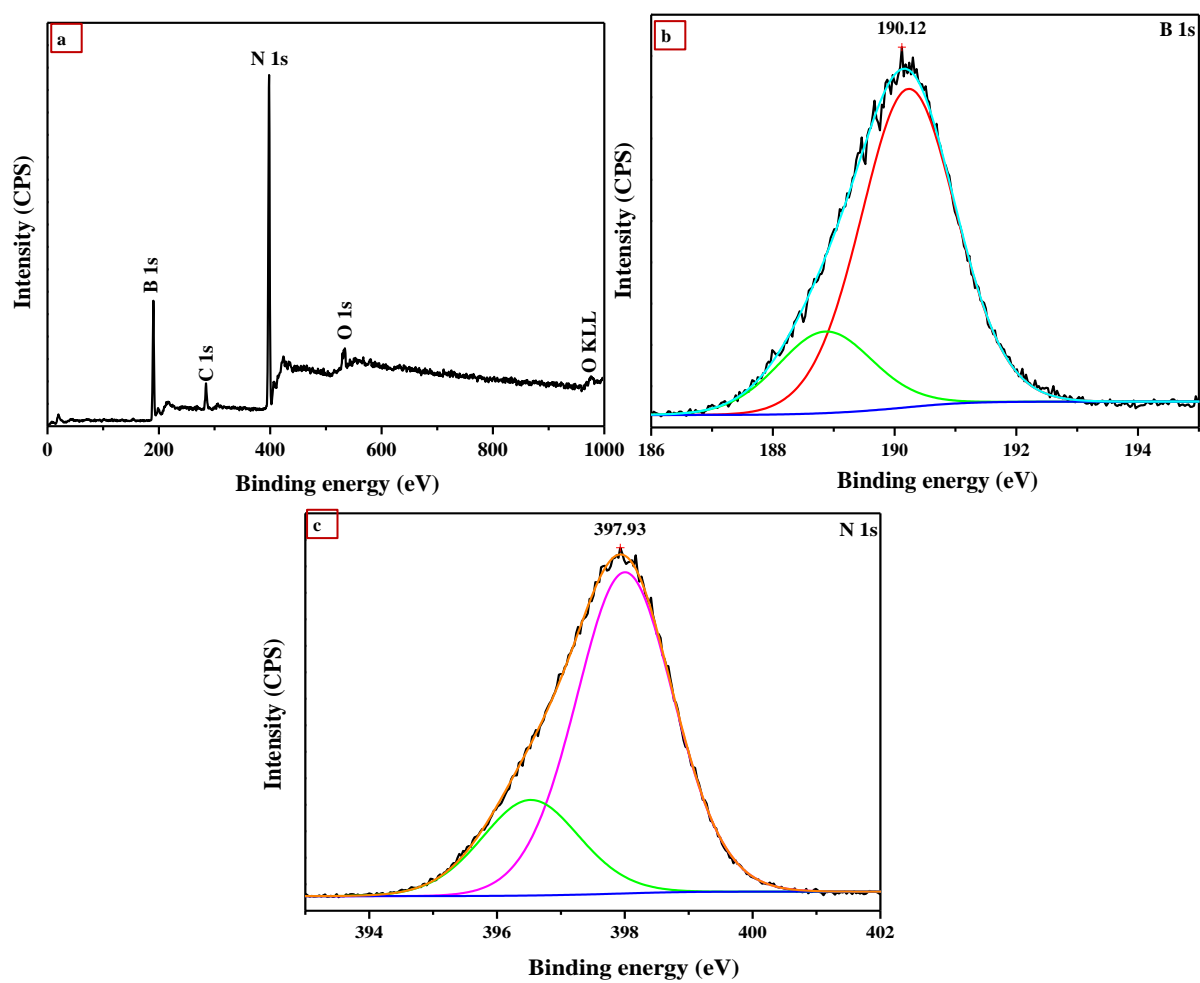
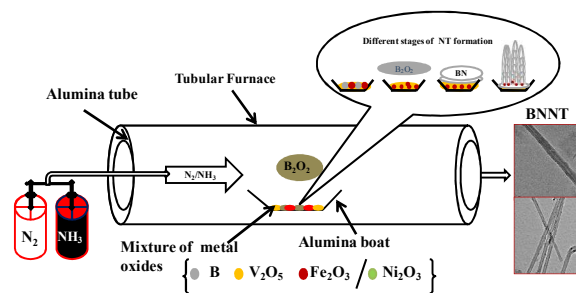


Fig. 10





TOC abstract: In this work the oxidizing efficiency of V_2O_5 is investigated on B/ Fe_2O_3 and B/ Ni_2O_3 system for BNNT synthesis via thermal CVD method.